Study of Switching Table Based DTC of Asymmetrical Dual 3-Phase Induction Machine

Manoj K Chaudhury[*1], Kali C Pradhan[1] Binay K Nayak[1] and Chinmay K Nayak[1]

Abstract

Multiphase drives offer pretty conspicuous benefits such as improvement of torque pulsation, reduction of rotor as well as dc-link current harmonics, reduction of phase current without affecting the phase voltage, improvement of reliability and power density. Thus, multiphase drives have been the epicentre of research in power electronics and drives. In this paper, the authors intend to obtain the dynamic d-q modelling of a Dual Three-Phase Induction Machine (DTIM). It delves into modelling of 6 phase SPWM, as well as open loop analysis of a DTIM fed from a SPWM inverter. The control techniques for the asymmetrical six-phase motor are somewhat different from that of its three-phase counterpart. Direct torque control technique is implemented as it is advantageous than the Indirect vector control technique from the perspective of increased cost and computational complexity.

Keywords: DTIM, DTC, SVPWM

1. Introduction

In contrast to past practices of strictly three-phase supply, inclusion of DC to AC converters for power supply eliminated the restrictions on number of phases an adjustable speed AC drive must have. Machines with more number of phases (more than three phases) came into picture as they pose the advantage of reducing the stress, in turn ratings of power electronics switches. Because, the control power is divided and distributed among more no. of inverter legs. This redundant structure helped in improving system level efficiency and power density. Multiphase induction machines are predominantly used in electric ship propulsion, traction and generally in high power applications [1].The DTIM consists of two windings spatially displaced by 30 degrees electrical and the two neutrals are isolated from each other. Ideally, it leads to six phase currents of equal amplitude [2].

However, their applications are still limited to the lower end of the high-power range due to the limitations on the ratings of the gate-turn-off-type semiconductor power devices. To achieve a high power rating in such systems, multilevel inverters have been developed in the past decade as a promising approach. Another strong contender in achieving high power is the multiphase-inverter-fed multiphase (in excess of three) induction machine drive system. In addition to enhancing the power rating, a multiphase system also has the merit of high reliability at the system level. In particular, with loss of one or more of the stator winding excitation sets, a multiphase induction machine can continue to be operated with an asymmetrical winding structure and unbalanced excitation.

Recently, several control techniques are considered about induction machines which application of each method depends on desired specific condition. One of these methods is called scalar and it is more suitable for low power applications [3]. In contrast, vector control of induction machines has better dynamic response. Despite of the higher phase number in multiphase induction machines, they have more degrees of freedom. Nevertheless, all these techniques are applicable for multiphase induction machines with little differences.

Direct Torque Control facilitates direct and independent control of motor torque and flux by selecting optimum inverter switching modes. The optimum voltage vector selection for the inverter is made so as to restrict the torque and flux errors within the hysteresis bands [4]. In [2], an overview on the state-of-the-art in the control of multi-phase drives employing dual-three phase induction machines is presented. In particular, focus is on modeling aspects, Pulse-Width Modulation (PWM) techniques for VSI, Field Oriented Control (FOC) and Direct Torque Control (DTC) strategies for dual-three phase induction machines. In [5], the recent progress in the design, modeling, and control, including healthy operation, of multiphase motor drives, and discusses open challenges and future research directions in the area are analyzed. In [6], an indirect field-oriented control (IFOC) scheme for a six-phase induction machine was modeled where the two three-phase winding sets are displaced randomly. The scheme has been proven to be easily extended to any number of phases, (multiples of three). A direct rotor-field-oriented control of a dual-three phase induction motor drive is described in [7, 8]. Three key issues like dynamic modeling of the machine using vector space decomposition (VSD) theory, use of double zero-sequence injection modulation technique and elimination of the innate asymmetries of drive's magnetic characteristics. In [9], vector control of a symmetrical six-phase induction machine with novel configuration is discussed. The aforementioned configuration is designed in a simple way that only three current sensors will be needed. A direct torque control (DTC) strategy equipped with features like constant inverter switching frequency, good transient and steady-state performance, and low distortion of machine currents is implemented for a DTIM drives in [10]. The advantages of the discussed control strategy are with respect to direct self-control (DSC) and other DTC schemes with variable switching frequency.

Experimental results are presented for a 10-kW DTC dual three-phase induction motor drive prototype. In [11], different hardware schemes of DTC are presented. One of the schemes takes the conventional switching table into consideration whereas the other does not. In [12], implementing and controlling a modified six-phase induction motor (MSPIM) is aimed at enhancement of motor reliability and reduction of torque pulsation. Non-linearities, including low order harmonics, cross-coupling saturation and iron losses cause deviations from the experimentally obtained waveforms. Thus, an improved version of VSD-based fractional order model of DTIM is proposed under both healthy and open circuit fault conditions. Optimization of the error between the simulated and experimentally obtained waveforms gives the apt differentiation orders [13]. In [14], different existing SVPWM techniques are analyzed for a dual three- phase induction motor (DTIM) supplied from two three- phase voltage source converters connected in parallel. A modified SVPWM method is also proposed for dual three- phase induction motor drive. Harmonic components in the phase currents and phase voltages are analyzed for all the four different SVPWM schemes. In [15], Common-mode voltage (CMV) produced by the two level six-phase voltage source inverter fed multi-phase machine is analyzed and a modified PWM technique is proposed for its reduction.

The electric drives used in industry are Adjustable Speed Drives and in most of these drives AC motors are applied. Induction motors are the standard in these drives. Induction motors are today the most widely used ac machines due to the advantageous mix of low cost, reliability and performance. So effective control of IM parameters e.g. speed, torque and flux is of utmost importance. From the investigation of the control methods it is known that torque control of IM can be achieved according to different techniques ranging from inexpensive Volts/Hz ratio strategy to sophisticated sensorless vector control scheme. But every method has its own disadvantages like losses, need of separate current control loop, coordinate transformation (thus increasing the complexity of the controller), torque and current ripple etc. So it is very much necessary to design a controller to obtain an ideal electric vehicle motor drive system which would have high efficiency, low torque ripple and minimum current distortion.

This paper aims to develop the mathematical modelling of dual three phase induction machine as well as designing a PWM inverter for six phase application for effective control of IM parameters e.g. speed, torque and flux is of utmost importance. From the investigation of various control methods, it has been observed that it is very much necessary to design a controller to obtain an ideal electric vehicle motor drive system which would have high efficiency, low torque ripple and minimum current distortion. Thus, direct torque control of dual three phase induction machine is explored.

The rest of the paper is organized as follows. Section II describes the modeling of the DTIM and the inverter. Section III sheds light on the proposed DTC scheme and the simulation results are presented and discussed in Section IV. Finally Section V concludes the research paper.

2. Mathematical Modelling of 6-Phase Induction Machine

The six stator phases are broken up into two wye-connected three-phase sets, each of which is labeled and has an axis offset by 30 degrees (set abc and set xyz). Each 3-phase set's windings are equally spaced and its axes are offset by 120 degrees. The three-phase rotor windings follow a sinusoidal pattern and have axes that are rotated by 120 degrees from one another.

Under these conditions, the vector space decomposition (VSD) method was employed to represent the 6-phase induction motor.

The rotor cage is comparable to a six-phase wound rotor, the windings are dispersed sinusoidally, and magnetic saturation and core losses are disregarded. Due to the use of full-pitch stator windings, there is no mutual leakage inductance in this machine.

The VSD states that the machine's initial six-dimensional (6-D) system can be split into three orthogonal subspaces (d,q), (z1,z2), and (o+,o-), with the resulting six-by-six transformation matrix (T6) exhibiting the following characteristics.

• Mapping the machine variables' fundamental components onto the harmonics of order k = 12n 1, (n = 1, 2, 3,...) in the (d,q) subspace. The air-gap flow is influenced by these factors.

• In the (z1,z2) subspace, harmonics of order k = 6n 1 (n = 1, 3, 5,...) undergo a transformation. Since the (d,q) and (z1,z2) subspaces are orthogonal, the air-gap flux is not affected by these harmonics (the 5th, 7th, 17th, 19th, etc.).

• A mapping exists between the (o+,o-) subspace and the zero-sequence components. Clarke's Transformation can be used to convert the stator voltages to d,q frame.

2.1 Modelling of DTIM using VSD method

The detailed modelling, based on VSD method is given in [15]. The stator voltage equation is

$$[v_s] = [R_s][i_s] + p([\lambda_s])$$

$$= [R_s][i_s] + p([\lambda_{ss}] + [\lambda_{sr}])$$

$$= [R_s][i_s] + p([L_{ss}][i_s] + [L_{sr}][i_r]) \ldots\ldots (1)$$

The rotor voltage equation is

$$[v_r] = [R_r][i_r] + p([\lambda_r])$$

$$= [R_r][i_r] + p([\lambda_{rr}] + [\lambda_{rs}])$$

$$= [R_r][i_r] + p([L_{rr}][i_r] + [L_{rs}][i_s]) \ldots\ldots (2)$$

The machine voltage equation in the d - q - z_1 - z_2 - $0_1 - 0_2$ subspace is presented below:

I) Machine Model in d-q subspace:

$$\begin{bmatrix} v_{ds}^s \\ v_{qs}^s \\ 0 \\ 0 \end{bmatrix} = \begin{bmatrix} r_s + L_s p & 0 & M_p & 0 \\ 0 & r_s + L_s p & 0 & M_p \\ M_p & \omega_r M & r_r + L_r p & \omega_r L_r \\ -\omega_r M & M_p & -\omega_r L_r & r_r + L_r p \end{bmatrix} \begin{bmatrix} i_{ds}^s \\ i_{qs}^s \\ i_{dr}^s \\ i_{qr}^s \end{bmatrix} \quad (3)$$

Where,

$$p = \frac{d}{dt}$$
$$L_s = L_{ls} + 3L_{ms}$$
$$L_r = L_{lr} + 3L_{ms}$$
$$M = 3L_{ms}$$

The torque developed in the machine is given by

$$T_e = \frac{1}{2}[i]^T \left(\frac{\partial}{\partial \theta_r}[L]\right)[i] \quad (4)$$

Which is simplified as

$$T_e = 3L_{ms}[i_{qs}^s[r_{dr}^r \cos(\theta_r) - r_{qr}^r \sin(\theta_r)) - i_{qs}^s[r_{dr}^r \sin(\theta_r) + r_{qr}^r \cos(\theta_r))] = 3L_{ms}\frac{P}{2}(i_{qs}^s i_{dr}^s - i_{ds}^s i_{qr}^s) \quad (5)$$

Where P, is the number poles in the machine.

2.2 Modelling of Inverters for Six-Phase Induction Machine

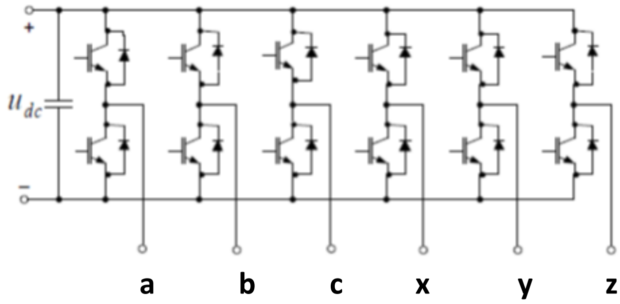

Fig. 1 : Six phase inverter

It can be assumed that there is no zero system voltage as long as the sum of stator currents is zero. Then the following relationship between bridge leg voltages and motor phase voltages is obtained:

$$v_{a_1}(t) = \frac{1}{3}\left(2v_{a_1N_1}(t) - v_{b_1N1}(t) - v_{c_1N1}(t)\right) \quad (6)$$

$$v_{b_1}(t) = \frac{1}{3}\left(2v_{b_1N1}(t) - v_{c_1N1}(t) - v_{a_1N_1}(t)\right) \quad (7)$$

$$v_{c_1}(t) = \frac{1}{3}\left(2v_{c_1N1}(t) - v_{a_1N_1}(t) - v_{b_1N1}(t)\right) \quad (8)$$

This implies that by controlling the inverter bridge leg voltages, the phase voltages of the machine can be controlled.

3. Switching Table based Direct Torque Control of DTIM

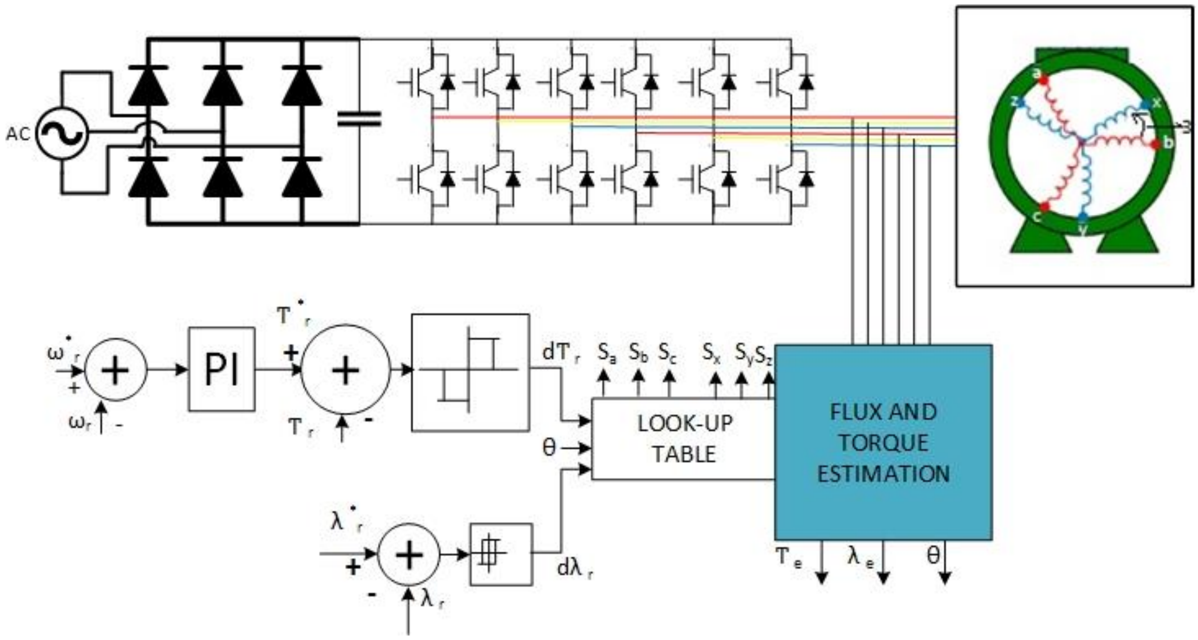

Fig. 2: Switching Table Based DTC

DTC controls motor flux and torque without rotor flux location. Finding the flux sector suffices. DTC aims to quickly decouple stator flux and electromagnetic torque. Hysteresis comparators of flux and torque and a switching logic table determine the inverter voltage vector (fig. 2). Multi-phase induction machines with multiple space voltage vectors provide additional inverter switching options. Unsuitable switching table selection causes high 6k ±1, (k = 1,3,...) harmonics at low speeds, reducing drive efficiency. K. Hatua, et al. [15] use flux control to decrease harmonics in the DTC of a six-phase induction machine. This method uses two different two-level flux hysteresis controllers for two stator fluxes (s1, s2). [17] suggests studying the switching table DTC of a six-phase induction motor. Due to the tiny stator impedance of the (z1−z2) domain, voltage harmonics of the order 6k ± 1 (k = 1,3,...) yield enormous stator current harmonics. Previous papers in this subject did not use an ideal switching table. The improper switching table selection in [18] causes a substantial torque ripple and loss in the (z1 −z2) domain. Table 3 shows how torque and stator flux errors determine vector selection in different solutions. Assuming the stator flux space vector in the (α −β) subspace is in sector k (k=1,..., and 12). Selecting voltage space vectors v_k, v_{k+1}, v_{k-2} raises flux magnitude, while v_{k+4}, v_{k+6}, v_{k-5} decreases it. Zero-voltage space vectors do not alter stator flux. Table 1 voltages minimize switching loss. (2) yields stator flux:

$$\psi_{s\alpha} = \int (V_{s\alpha} - R_s i_{s\alpha})\, dt \qquad (9)$$

$$\psi_{s\beta} = \int \left(V_{s\beta} - R_s i_{s\beta}\right) dt \qquad (10)$$

Table 1: Switching Table

		Sector Number											
ΔT	Δλ	1	2	3	4	5	6	7	8	9	10	11	12
1	1	2	3	4	5	6	7	8	9	10	11	12	1
	0	5	6	7	8	9	10	11	12	1	2	3	4
0	1	0	7	63	54	0	7	63	54	0	7	63	54
	0	7	63	54	0	7	63	54	0	7	63	54	0

	1	11	12	1	2	3	4	5	6	7	8	9	10
-1	0	8	9	10	11	12	1	2	3	4	5	6	7

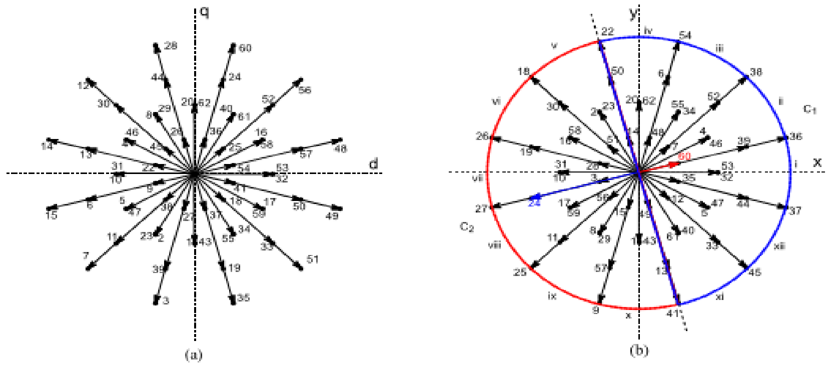

Fig. 3: Projections of voltage vectors in (a) dq subspace (b) xy subspace

In Fig. 3, a six-phase inverter delivers 48 independent nonzero vectors and one zero vector to build a 12-sided four-layer polygon in each machine subspace. The DSC and ST-DTC suffer from the relatively high harmonic content of phase currents due to current harmonics created in the (μ1, μ2) subspace, even though they have more voltage vectors than three-phase inverters. Thus, driving efficiency decreases. The schematic block diagram was used to model a DSC system for the dual three-phase induction machine prototype.

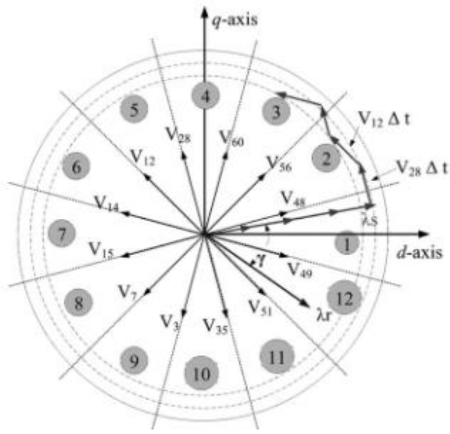

Fig. 4: DTC flux and torque hysteresis loop presentation

In Table 1 switching numbers minimize amplitude in the (z1 − z2) subspace. To reduce flux and torque errors, the stated DTC approach in fig 2 requires altering table rules. The switching table should reduce power loss in the (z1 − z2) subspace to increase motor efficiency. Fig. 2 shows a 6PIM with DTC and speed control.

The electromagnetic torque produced due to the interaction of stator and rotor flux is obtained by rearranging and substituting in equation (12), we get,

$$T_e = \frac{6}{2}\frac{p}{2}\frac{L_m}{\sigma L_{ls} L_{lr}} \lambda_s \lambda_r \sin\gamma \qquad (1)$$

The position of the stator flux is estimated using the following equation:

$$\theta = \tan^{-1}\frac{\lambda_{qs}}{\lambda_{ds}} \qquad (12)$$

Based on the position of estimated stator flux, the d-q plane is divided into 12 sectors. The generalized expression for sector k:

$$-\frac{\pi}{12}+\frac{\pi}{6}(k-1) \leq \theta < \frac{\pi}{12}+\frac{\pi}{6}(k-1), k = 1,2,\dots 12 \quad (13)$$

From the Eq. (13), torque varies as the angle between stator flux and rotor flux is changing, that is, γ. So in order to obtain high dynamic performance, it is required to vary c rapidly. In stationary reference frame, the stator flux equation can be written as:

$$\lambda_s = \int (V_s - R_s i_s)\, dt \quad (14)$$

If the stator resistance drop is neglected for simplicity, the stator flux varies along the direction of applied voltage vector and the Eq. (14) is reduced to

$$\lambda_s = v_s T_s + \lambda_s|_{t=0} \quad (15)$$

3.1 Direct Torque Control Simulation

Simulation follows mathematical modeling and control analysis. A stator voltage vector Vs applied for a short time interval Ts can incrementally adjust λs can be changed in steps to control γ. The command value of the stator flux vector $\lambda_s{}^*$depicts a circular trajectory while λ_s tracks the command flux in a zigzag path but confined to the hysteresis band as illustrated in Figure 4, introducing harmonics on the x-y plane. A hysteresis flux controller receives the flux error from comparing the stator flux reference to $\lambda_s{}^*$. The hysteresis torque controller input receives the difference between Te* and Te. These controllers' torque status dTe and flux status dF outputs are defined as:

$$dT_e = \begin{cases} 1, & Torque\ to\ be\ increased \\ -1, & Torque\ to\ be\ decreased \\ 0, & Torque\ remain\ unchanged \end{cases} \quad (16)$$

$$d\lambda = \begin{cases} 1, & Flux\ to\ be\ increased \\ 0, & flux\ to\ be\ decresed \end{cases} \quad (17)$$

The following setting are used during the simulation:

Flux band width	0.01wb
Torque bandwidth	0.1Nm
Sampling frequency	10kHz
Execution speed of PI loop	500Hz

4. Result and Discussion

The DTIM is simulated with the parameters mentioned in Table 2. The open loop response of the machine is mentioned in Figure 5. The machine is loaded with a load torque of 5 Nm at t=0.6 sec when the speed drops from 1500 rpm to 1410 rpm. The settling time during no load for speed is 0.15sec. From this it can be realized that the machine performs satisfactorily.

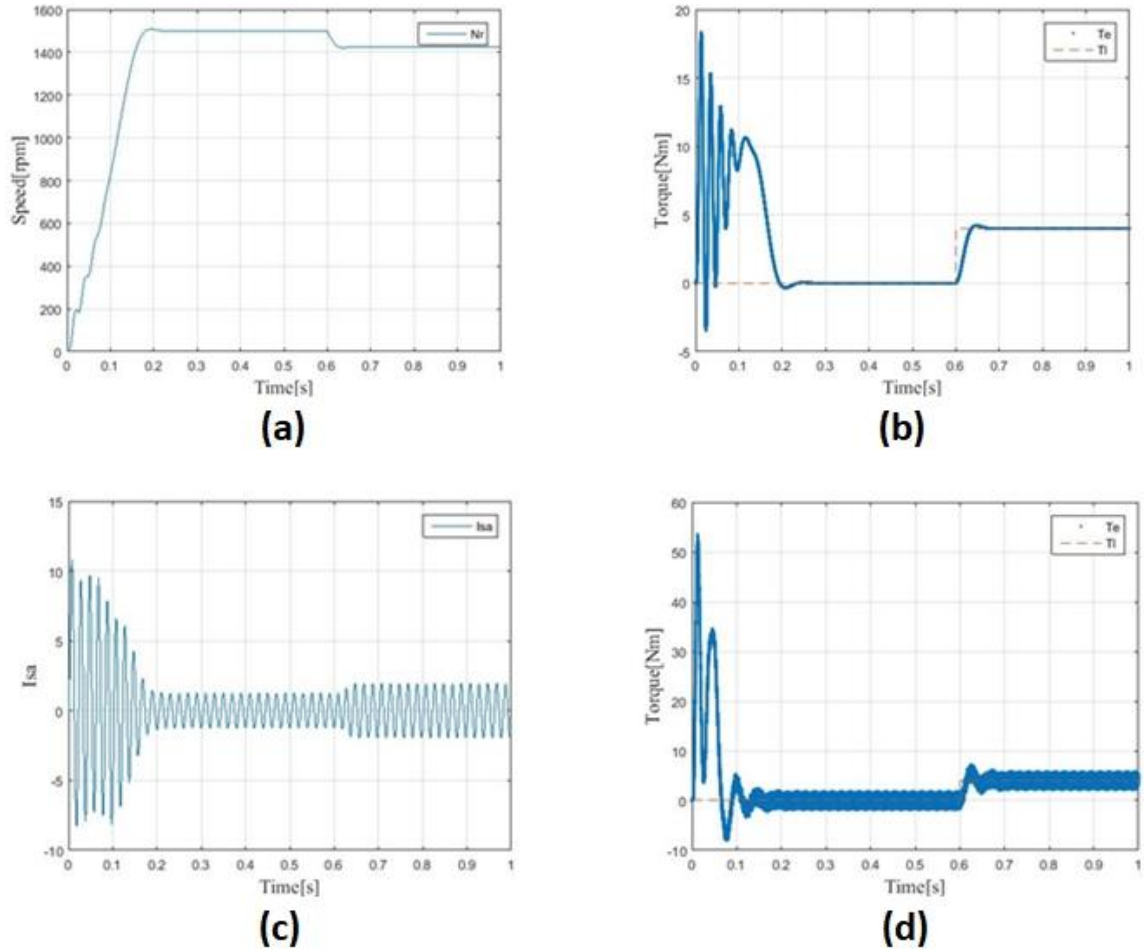

Fig. 5: Open loop response of the DTIM (a) Speed , (b) Developed torque (DOL mode), (c) Phase current, & (d) Developed torque (with SPWM)

Table 2: Machine parameters for simulation

Parameter	**Value**	**Parameter**	**Value**
Reference speed (K)	0.8	Pole Pairs (P)	2
Stator resistance in ohms (R_s)	11.6	Nominal frequency in Hz (F)	50
Rotor resistance in ohms (R_r)	10.4	Nominal power in watt (P_n)	750
Stator inductance in Henry (L_s)	0.579	Nominal speed in rpm (N_n)	1410
Rotor inductance in Henry (L_r)	0.579	Nominal phase voltage in volt (V)	220
Mutual inductance in Henry (L_m)	0.557	Stator leakage inductance in Henry (L_{gamas})	0.045
Inertia in kgm^2 (J)	0.002	Rotor leakage inductance in Henry (L_{gamar})	0.04

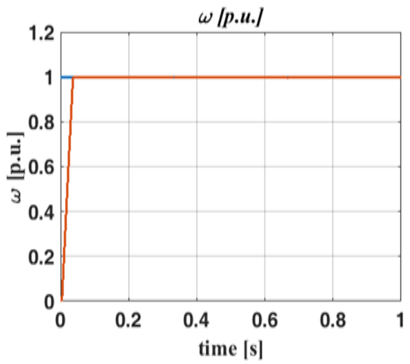

(a)

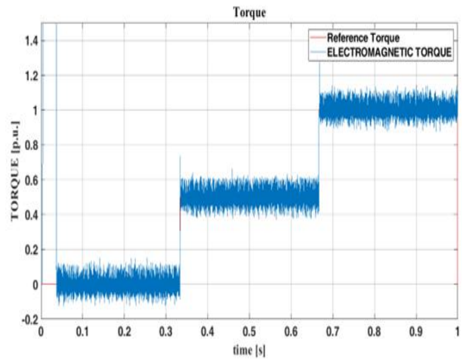

(b)

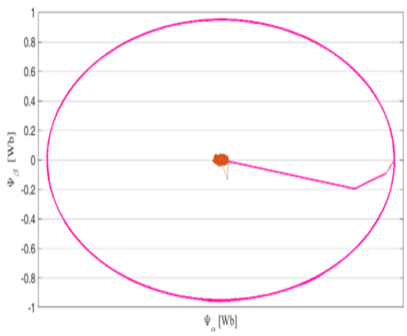

(c)

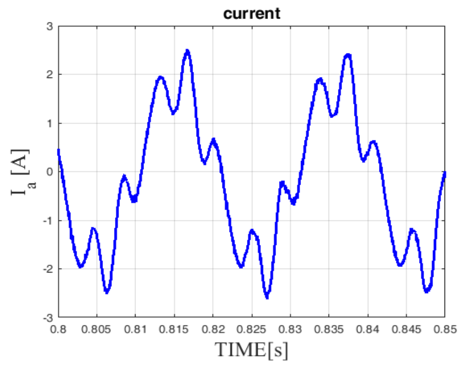

(d)

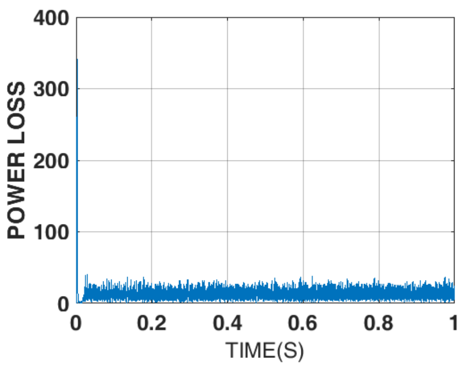

(e)

Fig. 6: DTC simulation results (a) Speed (b) Torque (c) Flux in α-β plane (d) Phase Current (e) Power loss

Switching table-based DTC simulation is carried out as per the parameters given in Table 2. The performance of the machine is depicted in fig. 6. The machine is operated at constant speed (Fig.6(a)) at different load torques (Fig.6(b)) The developed torque is seen to be closely following the reference torque. In a steady state condition, the DTIM is operated at 1410 RPM and 0, 0.5 and 1 p.u loading. The FFT results show that harmonic of the order 6k ±1 (k ¼ 1, 3, 5…) is present in the stator when the machine is operated using conventional DTC. The dynamic response of the studied control method can be seen from the figure 6. (c). the change in torque demand converges fast enough as was observed from the speed plot also.

Conclusion

Dual 3-phase induction machine is modelled using the VSD approach. The performance of the machine is studied first with direct supply, Subsequently, a SVPWM technique-based switching table is developed to meet the torque demand considering minimum error between the desired voltage and voltage vector. The Switching table based Direct Torque Control of Asymmetric Dual 3-phase induction Motor is carried out in this work. The torque ripple and current ripple are also minimised to a great extent by this method.

References

[1] G.K. Singh, "Multi-phase induction machine drive research – a survey", Electric Power Systems Research, Vol. 61, No. 2, pp. 139–147, 2002

[2] Bojoi, Radu, et al. "Dual-three phase induction machine drives control—A survey." IEEJ Transactions on Industry Applications 126.4 (2006): 420-429.

[3] I. Kioskeridis, N. Margaris, "Loss minimization in scalar-controlled induction motor drives with search controllers", *IEEE Transactions on Power Electronics*, Vol. 11, No. 2, pp. 213 – 220, 1996.

[4] Zhifeng Zhang, Renyuan Tang, "Novel Direct Torque Control Based on Space Vector With Modulation Adaptive Stator Flux Observer for Induction Motors", *IEEE Transactions on Magnetics*, Vol. 46, No. 8, August 2010.

[5] F. Barrero and M. J. Duran, "Recent Advances in the Design, Modeling, and Control of Multiphase Machines—Part I," in *IEEE Transactions on Industrial Electronics*, vol. 63, no. 1, pp. 449-458, Jan. 2016, doi: 10.1109/TIE.2015.2447733.

[6] G. K. Singh, K. Nam, Member, IEEE, and S. K. Lim, Student Member, IEEE, "A Simple Indirect Field-Oriented Control Scheme for Multiphase Induction Machine", IEEE Transactions On Industrial Electronics, Vol. 52, No. 4, August 2005.

[7] R. Bojoi, M. Lazzari, F. Profumo and A. Tenconi, "Digital field-oriented control for dual three-phase induction motor drives," in *IEEE Transactions on Industry Applications*, vol. 39, no. 3, pp. 752-760, May-June 2003, doi: 10.1109/TIA.2003.811790.

[8] R. Bojoi, F. Farina, G. Griva, F. Profumo and A. Tenconi, "Direct torque control for dual three-phase induction motor drives," in IEEE Transactions on Industry Applications, vol. 41, no. 6, pp. 1627-1636, Nov.-Dec. 2005, doi: 10.1109/TIA.2005.858281.

[9] H. P. Nabi, P. Dadashi and A. Shoulaie, "A novel structure for vector control of a symmetrical six-phase induction machine with three current sensors," 2011 10th International Conference on Environment and Electrical Engineering, 2011, pp. 1-5, doi: 10.1109/EEEIC.2011.5874735.

[10] E. Levi, R. Bojoi, F. Profumo, H.A. Toliyat and S. Williamson, "Multiphase induction motor drives – a technology status review", *IET Electric Power Applications*, Volume 1, Issue 4, July 2007, p. 489 – 516, DOI: 10.1049/iet-epa:20060342.

[11] Bibhu Prasad Panigrahi, Dinkar Prasad, Sabyasachi SenGupta, A simple hardware realization of switching table based direct torque control of induction motor, Electric Power Systems Research, Volume 77, Issue 2, 2007, Pages 181-190, ISSN 0378-7796, https://doi.org/10.1016/j.epsr.2006.02.015.

[12] Abdelwanis, Mohamed & Rashad, Essam Eddin & Taha, Ibrahim & Selim, Fathalla. (2021). Implementation and Control of Six-Phase Induction Motor Driven by a Three-Phase Supply. Energies. 14. 10.3390/en14227798.

[13] A. M. Shata, A. S. Abdel-Khalik, R. A. Hamdy, M. Z. Mostafa and S. Ahmed, "Improved Mathematical Modeling of Six Phase Induction Machines Based on Fractional Calculus," in IEEE Access, vol. 9, pp. 53146-53155, 2021, doi: 10.1109/ACCESS.2021.3069963.

[14] K.A, Chinmaya & Singh, Girish Kumar. (2018). Experimental analysis of various space vector pulse width modulation (SVPWM) techniques for dual three- phase induction motor drive. *International Transactions on Electrical Energy Systems*. 29. 10.1002/etep.2678. June 2018, pp.1-15.

[15] M. K. Chaudhury, M. Kumar Pathak and G. K. Singh, "Space Vector PWM With Common-Mode Voltage Reduction for Six-Phase Drive," 2020 IEEE 9th Power India International Conference (PIICON), 2020, pp. 1-6, doi: 10.1109/PIICON49524.2020.9112946.

[16] Bojoi, Radu & Farina, Francesco & Profumo, Francesco & Tenconi, Alberto. (2006). Dual-Three Phase Induction Machine Drives Control---A Survey. *IEEJ Transactions on Industry Applications*. 126. 420-429. 10.1541/ieejias.126.420.

[17] F. Blaschke, “The Principle of field-orientation as applied to the new 'transvector' closed loop control system for rotating-field machines”, Siemens Review, Vol. 34, No.. 5, pp. 217-220, 1972.

[18] Giovanna Oriti and Alexander L. Julian, “Three-Phase VSI with FPGA-Based Multisampled Space Vector Modulation”, *IEEE transactions on industry applications*, Vol. 47, No. 4, July/August 2011.